J Electr Eng Technol Vol. 9, No. 1: 307-312, 2014
http://dx.doi.org/10.5370/JEET.2014.9.1.307

ISSN(Print) 1975-0102
ISSN(Online) 2093-7423

FE Analysis of Plasma Discharge and Sheath Characterization in Dry Etching Reactor

Gwang Jun Yu*, Young Sun Kim†, Dong Yoon Lee, Jae Jun Park**, Se Hee Lee*** and Il Han Park***

Abstract – We present a full finite element analysis for plasma discharge in etching process of semiconductor circuit. The charge transport equations of hydrodynamic diffusion-drift model and the electric field equation were numerically solved in a fully coupled system by using a standard finite element procedure for transient analysis. The proposed method was applied to a real plasma reactor in order to characterize the plasma sheath that is closely related to the yield of the etching process. Throughout the plasma discharge analysis, the base electrode of reactor was tested and modified for improving the uniformity around the wafer edge. The experiment and numerical results were examined along with SEM data of etching quality. The feasibility and usefulness of the proposed method was shown by both numerical and experimental results.

Keywords: Plasma discharge, Charge transport equation, Sheath characteristics, Dry etching, Finite element analysis

1. Introduction

Plasma etching and deposition are currently in widespread use in the manufacturing process of semiconductor circuit. Despite of the importance of plasma processing, however, a gas glow discharge is not well understood. This comes from the non-equilibrium nature of the plasma, and the complex interaction among potential field, transport phenomena, plasma chemistry, and surface reaction kinetics. Therefore, design of plasma reactor is still based on empirical approaches. Main requirements of plasma etching include high etching rate, uniformity, anisotropy, and selectivity [1]. However, it is very difficult to satisfy all of the above requirements simultaneously. In addition, as the wafer size continues to increase, it becomes more difficult to satisfy uniformity and anisotropy.

Recently, there has been increasing interest in developing mathematical models and numerical analysis of the plasma process in an effort to better understand the process and to improve the design of plasma reactors. The most frequently used algorithms are the hydrodynamic diffusion-drift model incorporating flux-corrected-transport (FCT) method and particle-in-cell (PIC) method [2-6]. In this paper, we proposed a full finite element approach where the charge transport equations of hydrodynamic diffusion-drift model and the electric field equation were numerically solved in a fully coupled system by using a standard finite element procedure for transient analysis[7-11]. Numerical technique for the hydrodynamic diffusion-drift modeling using charge transport equations is used in various applications such as corona discharge, heat transfer and cooling effect of heavy electric machines [12-14].

The proposed method was applied to a real plasma reactor in order to characterize the plasma sheath just above a targeted silicon wafer. The plasma sheath is closely related to the yield of the etching process since it accelerates the bombing ions, whose motional properties determine the etching quality such as uniformity and anisotropy. In this work the base electrode of the initial reactor was also modified to improve the edge effect deteriorating the uniformity, and its experiment results of etching quality were compared with ones of the initial one by examining data of SEM (scanning electron microscope).

2. Analysis Model of Dry Etching Chamber

Fig. 1 shows a cross-sectional diagram of the chamber for dry etching process. A wafer is placed between two electrodes. The upper electrode is connected to a voltage source and the lower one is set as ground. The electrodes supply external energy into the chamber for generating and sustaining the plasma. The electric field between the electrodes is downward and drives charge carries. The plasma sheath is formed just above the wafer and it accelerates heavy irons that bomb the wafer surface for etching. But the electric field above the wafer is not uniform in intensity and direction because of the fringing effect on the edge side.

† Corresponding Author: Dept. of Electrical and Electronic Engineering, Joongbu University, Geumsan, Korea. (yskim@joongbu.ac.kr)
* School of Electronic Electrical Engineering, Sungkyunkwan University, Suwon, Korea. (joonynet@naver.com, ihpark@skku.ac.kr)
** Dept. of Electrical and Electronic Engineering, Joongbu University, Korea. (dylee@joongbu.ac.kr , jjpark@joongbu.ac.kr)
*** Dept. of Electrical Engineering, Kyungpook National University, Daegu, Korea. (shlees@knu.ac.kr)
Received: September 12, 2012; Accepted: October 2, 2013

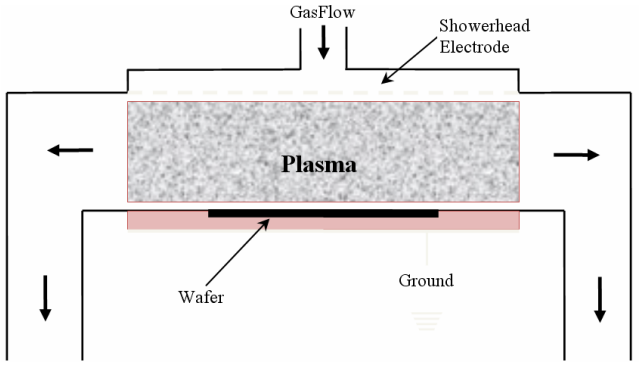

Fig. 1. Schematic view of wafer etching reactor. Plasma sheath is formed just above the wafer and it accelerates heavy ions that bomb the wafer surface. Electric field above the wafer is not uniform in intensity and direction because of the fringing effect around the edge side.

In this work, the uniformity of electric field was improved by substituting an existing quartz ring, which was located below the wafer, with an aluminum ring.

3. Hydrodynamic Diffusion-Drift Model for Discharge Process

The simplified expressions of governing equations for the plasma discharge can be analyzed by using the hydrodynamic diffusion-drift model for the concentration of the electron (N_e), positive ions (N_p), and neutral ions (N_n) as

$$\begin{aligned}
\frac{\partial N_e}{\partial t} + \nabla \cdot (N_e \mathbf{V}_e) &= S + N_n \alpha \,|\, \mathbf{V}_e \,| - N_e N_p \beta_{ep} \\
\frac{\partial N_p}{\partial t} + \nabla \cdot (N_p \mathbf{V}_p) &= S + N_n \alpha \,|\, \mathbf{V}_e \,| - N_e N_p \beta_{ep} \\
\frac{\partial N_n}{\partial t} + \nabla \cdot (N_n \mathbf{V}_n) &= S - N_n \alpha \,|\, \mathbf{V}_e \,| + \gamma
\end{aligned} \tag{1}$$

where t denotes the time, $\mathbf{V}_e$, $\mathbf{V}_p$, and $\mathbf{V}_n$ the electron, positive ion, and neutral ion drift velocities,and α, β and γ the material functions for theionization, recombination, and concentration of new supplied gas, respectively. S denotes the source term, and here its effect was neglected. Diffusion effect was also neglected because it doesn't have any significant effect [2]. We, however, used the artificial diffusion scheme to avoid the numerical discontinuity caused by the shock wave at the front of space charge propagation. These three given continuity equations were transformed by incorporating the artificial diffusion term and were then solved along with the Poisson's equation, resulting in new expressions for electric field distributions each time as exhibited by the following expression as

Table 1. Material functions [2, 4, 6]

Lists	Conditions
Electron velocity, Ve (cm/s)	-382E
Positive ion velocity, Vp (cm/s)	-3.42E
Secondary electron emission factor, (mol/m^2-s)	0.01 NpVp
α , (cm^{-1})	0.0035exp (-1.65*10^{5}E-1)
β , (cm^{-1})	2X10^{-7}

$$\nabla(-\varepsilon \nabla V) = e(N_p - N_e) \tag{2}$$

where ε is the dielectric permittivity, e the electron charge, and V the electric scalar potential.

Table 1 shows the material functions used in this simulation. The velocities of each carrier were expressed as the electric field dependent problem. The coupled parameter between charge continuity equations and Poisson's equation is the electric field intensity, **E**. Therefore, to analyze the plasma discharge process, those equations were fully combined with each other and solved simultaneously with each time step. The ion-secondary emission coefficient was employed as 0.01 which was estimated by von Engel [2].

4. Numerical and Experimental Results

4.1 2-D Axi-symmetrical analysis

To verify our numerical setup, we first tested 2-D analysis model of which the analysis conditions and the initial conditions are shown in Table 1, Table 2 and Table 3, respectively. While the electric field applied to this analysis region, the carriers flow along with the electric field line because this is electric field dependent problem as we can the governing equations, (1). Therefore, the positive ions move toward the lower electrode and the electron move toward the upper electrode. When the positive ions are induced and bombarded at the lower electrode, it generates an additional electron flux, called the secondary emission.

Fig. 1 shows the analysis model with 2-D axi-

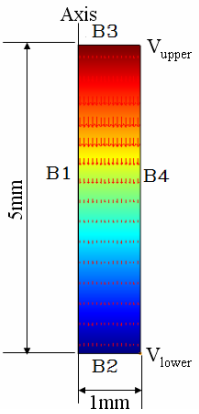

Fig. 2. 2-D axi-symmetrical model for plasma discharge.

symmetrical structure. The variation of electric scalar potential was depicted in Fig. 3. The distribution of the electric potential was linear at the initial time, but the potential in plasma region increased much higher than other electrodes with time. Because there was no more change in plasma region after $1e^{-4}$ (s), the plasma status was reached at a stable point. Fig. 4(a) shows the electron and ion densities after 1 (s). Except around electrodes, the neutral region can be viewed widely. Around the electrodes, the density of a positive ion was higher than that of electron, which is the plasma sheath region, as shown in Figs. 4(b) and 4(c). Because the electric potential in plasma region is higher than other places, the electric field will be formed and it accelerates the Argon ions toward the electrodes resulting in the secondary electron emission.

Table 2. Boundary conditions and initial values for 2-D axi-symmetrical analysis

Lists		Conditions
Gap distance between two electrodes		5 (mm)
Upper electrode		10 (V)
Lower electrode		0 (V)
Gas type		Argon
Pressure		10 (mTorr)
Boundary, B1	Electron	Axisymmetry
	Positive ion	Axisymmetry
	Neutral ion	Axisymmetry
Boundary, B2	Electron	Flux : 0.01*normE_es*NP*3.42+ normE_es*NE*382*(-1) mol/m^2-s
	Positive ion	Flux : normE_es*NP*3.42*(-1)mol/m^2-s
	Neutral ion	Insulation
Boundary, B3	Electron	Flux : normE_es*NE*382*(-1)mol/m^2-s
	Positive ion	Flux : normE_es*NP*3.42*(-1)mol/m^2-s
	Neutral ion	Insulation
Boundary, B4	Electron	Insulation
	Positive ion	Insulation
	Neutral ion	Insulation

NE: Electron density NP: Density of ion
NN: Density of neutral ion normE_es: Electric field

Table 3. Initial conditions for gases

Carrier	Initial concentration (mol/m^3)
Argon neutral gas	5.87e-4
Electron	5.87e-6
Argon positive ion	5.87e-6

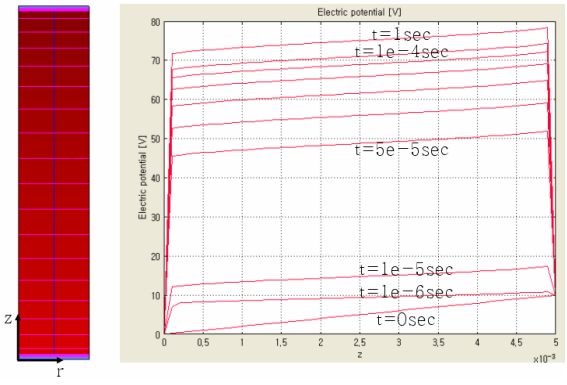

Fig. 3. Variation of electric potential as a function of time.

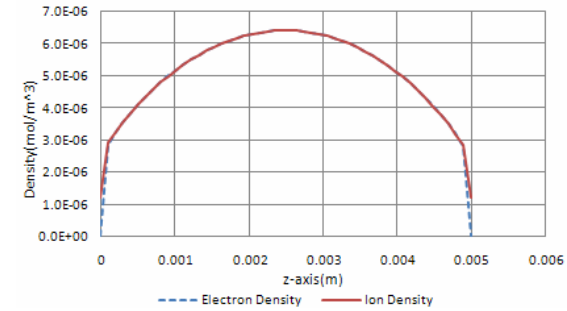

(a)

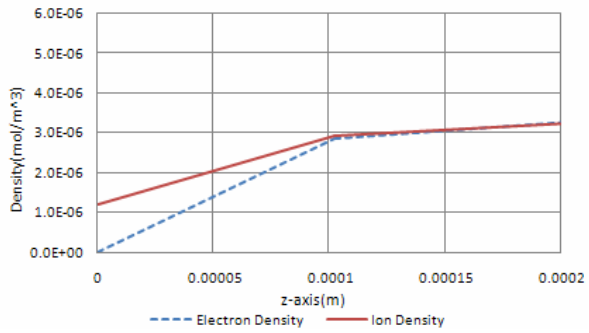

(b)

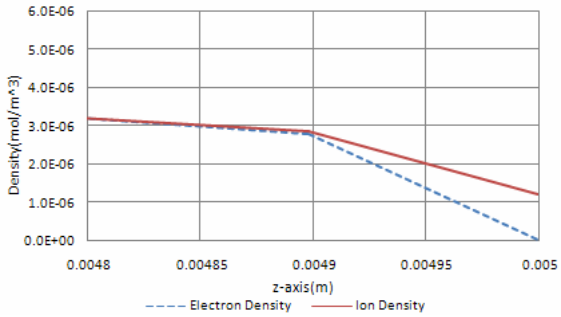

(c)

Fig. 4. Variations of negative electron and Ar ion (a) between the upper and lower electrode, (b) near lower electrode, and (c) near upper electrode.

4.2 Discharge analysis of dry etching chamber and experimental results

After verification the plasma process in two-dimensional problem, here, the proposed method was applied to axi-symmetric model with a real vacuum chamber as shown in Fig. 5. The distance between the wafer and the upper electrode was 30 (mm) and the diameter of wafer was 300 (mm).

The main issue is here to improve the etching process around wafer edge by using the discharge simulation. From the discharge analysis, this problem is strongly dependent on the velocity field which is composed of the mobility and

electric field. Therefore, the electric field distribution will be the most important factor to improve the uniformity in the wafer. Fig. 5 shows the electric field and potential distribution of the dry etching chamber. As we can see the Fig. 7(a), the etching process was good enough at the center of wafer because of directly injected electric field. On the contrary, the etching process around the wafer edge, shown in Fig. 7(b), should be modified with enhancing the electric field. From this, we concluded that the electric field injection angle guiding the ionized particles should be modified around the edge. Non-uniformity is effected by a large electrical resistance(low electrical conductivity) for quartz block. Radial components of electric potential distribution on etching target with the radius and trend line for)quartz and aluminum block are shown in Fig. 8.

The degree of parallelization of eq-potential line and upper side of the etching target is improved when the Q1 block is aluminum. So, an incidence angle is changed to 2(deg) from existing 6(deg.).

Therefore, we replaced the quartz with aluminum as shown in Fig. 9 and Fig. 10. Fig. 9 shows the SEM images

Table 4. Electrical properties for block

Material	Electrical conductivity	Relative permittivity
Aluminum	3.55e+7 S/m	1
Silicon	1.0e-12 S/m	12.1
Quartz	0.0 S/m	4.3

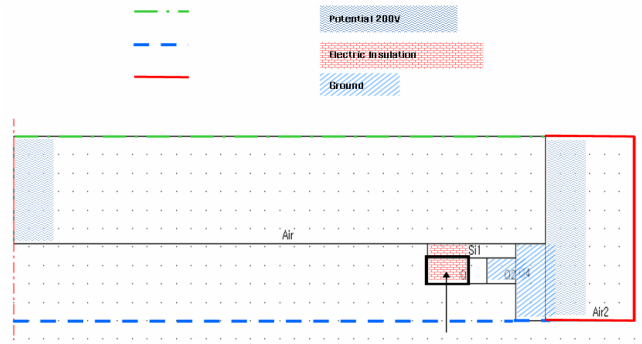

Fig. 5. Axi-symmetric model with dry etching chamber. and design variables.

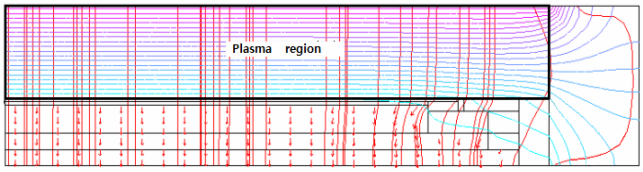

Fig. 6. Electric field and eq-potential distribution for dry etching chamber.

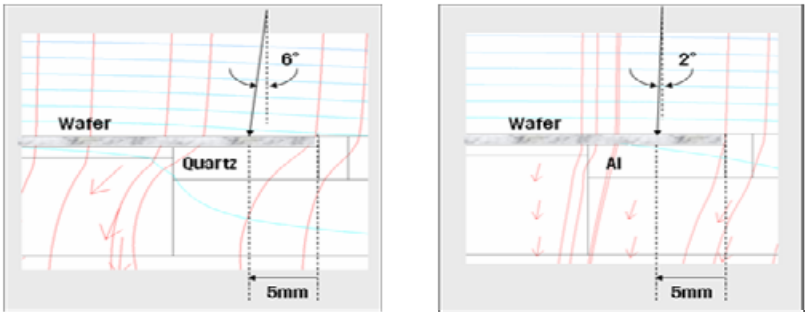

(a) (b)

Fig. 7. Comparison of electric field distributions when the Q1 block is (a) quartz and (b) aluminum ring.

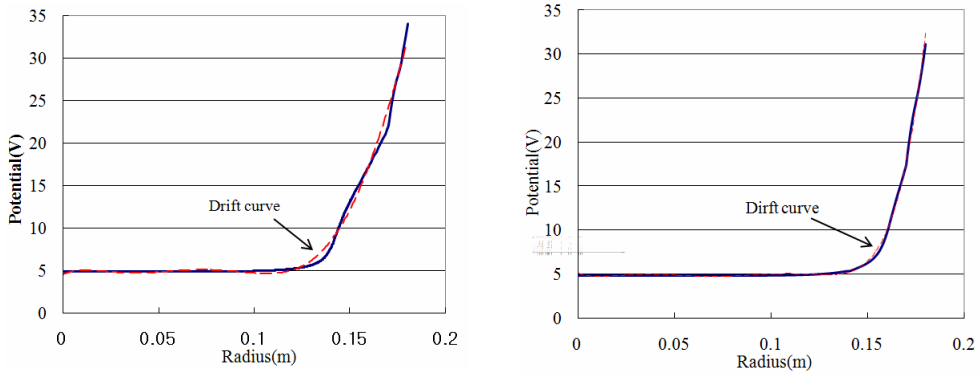

(a) (b)

Fig. 8. Radial component of electric potential distribution on etching target with the radius and trend line for (a) quartz and (b) aluminum block.

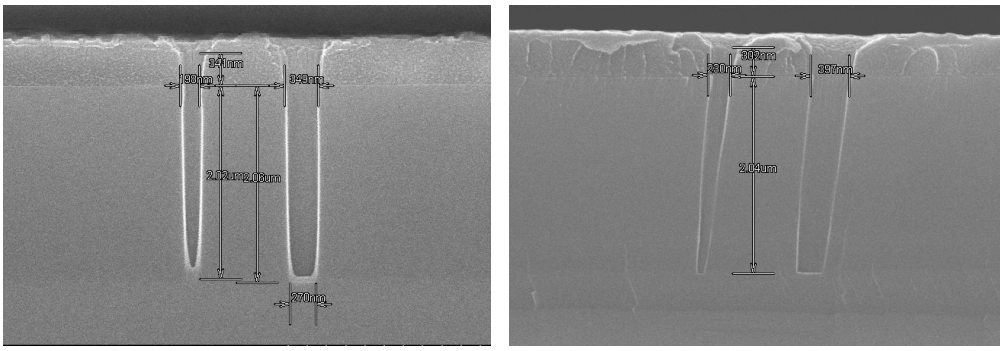

(a) (b)

Fig. 9. SEM images of wafer trench in the existing quartz block (a) wafer center, and (b) wafer edge.

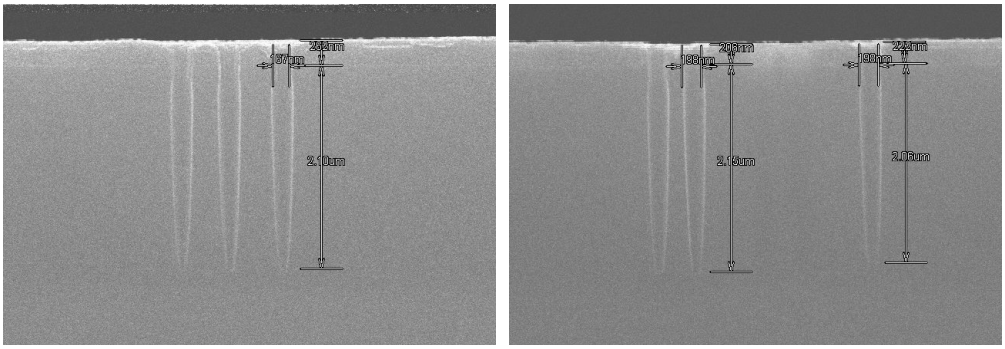

(a) (b)

Fig. 10. SEM images of wafer trench in the improved aluminum block (a) wafer center, and (b) wafer edge.

of wafer trench in the existing quartz block at the wafer center and wafer edge. After this modification, the uniformity of electric field near wafer edge was improved. The SEM images of wafer trench with the improved aluminum block show the dramatic enhancement in etching process as shown in Figs. 10(a) and 10(b).

5. Conclusion

We presented a full finite element analysis for plasma discharge in etching process of semiconductor circuit. The charge transport equations of hydrodynamic diffusion-drift models and the electric field equation were numerically solved in a fully coupled system. A plasma reactor was analyzed and was newly designed to improve the uniformity of etching. To decreasing the edge effect due to field fringing, Q1 block material was changed from Quartz(dielectric) to Aluminum(conductor). SEM data showed the improved etching quality on the edge side of wafer. The feasibility and usefulness of the proposed method was shown by both numerical and experimental results. Also, more detail issues like design technique for reactor will be suitable for another version.

Acknowledgment

This work was supported by Basic Science Research Program through the National Research Foundation of Korea(NRF) funded by the Ministry of Education (2013R1A2A2A01010327).

References

[1] Antonios Armaou, James Baker, and Panagiotis D. Christofides, “Feedback control of plasma etching reactors for improved etching uniformity,” *Chemical Engineering Science*, vol. 56, pp. 1467-1475, 2001.

[2] R. Morrow, “Theory of negative corona in oxygen,” *Phys. Rev. A*, vol.32, no. 3, pp. 1799-1809, 1985. G. Steinle, D. Neundorf, W. Hiller, and M. Pietralla, “Two-dimensional simulation of filaments in barrier discharges,” *J. Phys. D: Appl. Phys.*, vol. 32, pp. 1350-1356, 1999.

[3] J. Paillol, P. Espel, T. Reess, A. Bibert, and P. Domens, “Negative corona in air at atmospheric pressure due to a voltage impulse,” *J. Appl. Phys.*, vol. 91, no. 9, pp. 5614-5621, 2002.

[4] G. E. Georghiou, A. P. Papadakis, R. Morrow, and A. C. Metaxas, “Numerical modeling of atmospheric pressure gas discharges leading to plasma pro-

duction," *J. Phys. D: Phys*., vol. 38, pp. R308-R328, 2005.
[5] S. Ethier, W. M. Tang, Z. Lin, "Gyrokinetic particle-in-cell simulations of plasma microturbulence on advanced computing platforms," *Journal of Physics: Conference Series,* vol. 16, pp. 1-15, 2005.
[6] Se-Hee Lee, Se-Yeon Lee, and Il-Han Park, "Finite Element Analysis of Corona Discharge Onset in Air with Artificial Diffusion Scheme and under Fowler-Nordheim Electron Emission Condition," *IEEE Trans. Magn.*, vol. 43, no. 4, pp. 1453-1456, April, 2007.
[7] Woong-Gee Min, Seok-Hyun Lee, Hyoeng-Seok Kim, and Song-Yop Hahn, "Transient Approach to Steady State of Discharge Phenomena in Corona Device," *IEEE Trans. Magn*., vol. 38, no. 2, pp. 485-488, March, 2002.
[8] Jae Hak Shim, Seung Kil Choi, Hui Dong Hwang, Duk Yong Ha, Kwang Cheol Ko, and Hyung Boo Kang, "2-D Simulation on the Corona Discharge of Negative Needle-to-Plane Electrodes," *IEEE Trans. Magn*., vol. 38, no. 2, pp. 1181-1184, March, 2002.
[9] Pierre Atten, Jean-Louis Coulomb, and Bassem Khaddour, "Modeling of Electrical Field Modified by Injected Space Charge," *IEEE Trans. Magn.*, vol. 41, no. 5, pp. 1436-1439, May, 2005.
[10] Bassem Khaddour, Pierre Atten, and Jean-Louis Coulomb, "Numerical Solution and Experimental Test for Corona Discharge Between Blade and Plate," *IEEE Trans. Magn*., vol. 43, no.4, pp. 1193-1196, April, 2007.
[11] Bassem Khaddour, Pierre Atten, and Jean-Louis Coulomb, "Electrical Field Modified by Injected Space Charge in Blade-Plate Configuration," *IEEE Trans. Magn*., vol. 42, no. 4, pp. 651-654, April, 2006.
[12] Y.K. Stishkov and V. A. Chirkov, "Formation of electro hydrodynamic flows in strongly nonuniform electric fields for two charge-formation modes," *Tech. Phys*., vol. 57, no. 1, pp. 1-11, 2012.
[13] T. Lu, G. Xiong, X. Cui, H. Rao, and Q. Wang, "Analysis of corona onset electric field considering the effect of space charges," *IEEE Trans. Magn*., vol. 47, no. 5, pp. 1390-1393, May 2011.
[14] J. G. Hwang et al., "Effects of nanoparticle charging on streamer development in transformer oil based nanofluids," *J. Appl. Phys*., vol. 107, no. 1, p. 014310, 2010.

Gwang Jun Yu He received the MS in Electrical Engineering from the SKKU, Korea, in 2009. He is a senior engineer of Global Production Technology center, Samsung Electronics.

Young Sun Kim He received the MS and the PhD in Electrical Engineering from the Dankook University of Seoul, Korea, in 1997 and 2006, respectively. He was a postdoctoral fellow of MIT in 2010-2011, He is a professor of Joongbu University and his academic interests are analysis and optimal design of multi-physics system based on electromagnetic field.

Dong Yoon Lee He received the M.S degree in Electrical Engineering and the Ph.D degree in Electrical Electronic Engineering from Yonsei University, Seoul, South Korea, in 1990 and 2001, respectively. He is currently a professor with Joongbu University, Chungnam, South Korea. His research interests include security system, artificial intelligence and application.

Jae Jun Park He received MS and PhD degrees in Electrical Engineering from Kwangwoon University in 1987 and 1993, respectively. He is currently a Professor at Joongbu University from 1997 and his present academic interests are in electrical insulation and diagnosis of electric power facilities.

Se Hee Lee He received his B.S. and M.S. degrees in electrical engineering from Soongsil University, Seoul, Korea, in 1996 and 1998, respectively. He received his Ph.D. degree in electrical and computer engineering from Sung-kyunkwan University in 2002. He performed postdoctoral research at Massachusetts Institute of Technology (MIT) and worked for the Korea Electrotechnology Research Institute (KERI) before joining the faculty of Kyungpook National University in the School of Electrical Engineering and Computer Science in 2008. His research interests focus on the analysis and design of Electromagnetic Multiphysics problems spanning the macro- to nano-scales.

Il Han Park He received MS and PhD degrees in Electrical Engineering from Seoul National University in 1986 and 1990, respectively. He is a Professor at Sungkyunkwan University and his present academic interests are in electromagnetic force and its multiphysics problems coupled with fluid, micro-particle, mechanical dynamics, heat transfer and electric discharges.